Proc. VIIth Digital Image Computing: Techniques and Applications, Sun C., Talbot H., Ourselin S. and Adriaansen T. (Eds.), 10-12 Dec. 2003, Sydney

Compression of Dynamic PET Based on Principal Component Analysis and JPEG 2000 in Sinogram Domain

Zhe Chen[1] and David Dagan Feng[1,2]

[1] Biomedical and Multimedia Information Technology (BMIT) Group
School of Information Technologies, The University of Sydney
zhechen@it.usyd.edu.au
feng@it.usyd.edu.au
[2] Center for Multimedia Signal Processing (CMSP),Department of Electronic & Information Engineering,Hong Kong Polytechnic University

Abstract. A new algorithm for the compression of dynamic positron emission tomography (PET) data is presented. It consists of a temporal compression stage based on the application of principal component analysis (PCA) directly to the PET sinograms to reduce the dimensionality of the data. This is followed by a spatial compression stage using JPEG 2000 to each PCA channel weighted by the signal in each channel. By combining these temporal and spatial compression techniques we can achieve a compression ratio as high as 129:1 while simultaneously reducing noise and improving functional estimation compared with the uncompressed data, and preserving the sinogram data for later analysis. We validate our approach with a simulated phantom FDG brain study and clinical dynamic PET datasets. The results of performance evaluation suggest the new compression technique not only is able to reduce the original sinogram datasets by more than 95%, but also improve the reconstructed image quality for the quantitative analysis.

1 Introduction

Positron emission tomography (PET) raw data are initially acquired as projection data in the form of sinograms, which require large volumes of data storage. For example, a dynamic PET study using a SIEMENS ECAT 951R PET scanner consist of 31 cross-sectional planes, each of which has 22 temporal frames, and each sinogram frame has 192 x 256 pixels. However, the original large volume of sinograms may not be necessary to provide the maximum information for the study. It is desirable for the sinograms to be compressed while preserving reconstructed image fidelity before being transmitted and stored. In our previous work, we have demonstrated a new temporal compression scheme based on the application of principal component analysis (PCA) [1] directly to PET sinograms prior to image reconstruction (S-PCA) [2]. It can reduce the dimensionality of the data from typically 22 to 5 temporal frames, whilst simultaneously reducing noise and improving functional estimation compared with the original data. Additionally it

avoids introducing image reconstruction errors into the analysis and decreases the computational burden of image reconstruction. Moreover, the S-PCA helps to extract the useful information from the PET, producing more precise functional modeling comparing with a conventional sampling schedule (CSS), an optimal sampling schedule design (OSS), and the PCA in image domain (I-PCA) [2]. In this paper, we extend the temporal compression algorithm by combining the S-PCA and channel-weighted JPEG2000 in the sinogram domain with the dual aims of diagnostic accuracy and high compression ratios. Some investigators have previously applied PCA and DCT such as JPEG in the image domain as the data compression technique for dynamic medical imaging [3,4]. However, JPEG can create blocking artifacts at high compression ratios, which can affect the reconstruction. In this paper we will systematically analyse the performance of the new compression method based on PCA with JPEG 2000 in the sinogram domain (S-PCA + S-JPEG2000) using the Zubal phantom simulation data [5] and three clinical patient studies. We compare the results of the estimation of local cerebral metabolic rate of glucose (LCMRGlc) using a five-parameter glucose tracer ^{18}*F-fluoro-deoxyglucose* (FDG) model [6] on the decompressed sequence, as such quantitative analysis of dynamic PET is a key requirement [7].

2. Dynamic PET with Tracer Kinetic Modeling

The term functional imaging refers to a range of measurement techniques in which the aim is to extract quantitative information about physiological function from image-based data. Unlike the anatomical imaging techniques which provide structural information, biomedical functional imaging techniques such as PET and SPECT can provide image-wide quantification of physiological, pharmacological and biochemical functions within the body, and support the visualization of the distribution of these functions corresponding to anatomical structures. Physiological function can be estimated by observing the behaviour of a small quantity of an administered substance 'tagged' with radioactive isotopes. Images are formed by the external detection of gamma rays emitted from the patient when the radioactive isotopes decay. Because they allow observation of the effects of physiological processes, functional imaging techniques can provide unique diagnostic information. Tracer kinetic modeling techniques are widely applied in PET to extract physiological information about dynamic processes in the human body. Generally, this information is defined in terms of a mathematical model $\mu(t|P)$ (where $t=1,2,\ldots,T$ are discrete sampling times of the measurements and P is a set of model parameters), whose parameters describe the delivery, transport and biochemical transformation of the tracer. The input function for the model is the plasma time activity curve (PTAC) obtained from the measurement of blood samples. Reconstructed PET images provide the output function in the form of a physiological tissue time activity curve (TTAC) denoted by $Z_i(t)$, and $i=1,2,\ldots,I$ corresponds to the *i*-th pixel in the imaging region. Application of the model on a pixel-by-pixel basis to measured PTAC and TTAC data using known rapid parameter estimation algorithms, yields physiological parametric images.

3 Method

Our compression method has the following major steps:
Compression stage: Step1. Noise normalization of PET sinogram frames; Step 2. PCA is applied to the noise-normalized sinograms; Step 3. The compression ratios for each channel are determined based on the signal importance in each channel; Step 4. Channel-weighted JPEG 2000 is applied to each sinogram principal component channel.
Decompression stage: Step 5. JPEG 2000 is decoded to regenerate decompressed sinogram PCs; Step 6. Sinogram PCA channels are reconstructed e.g. using filtered-back projection; Step 7. Inverse PCA is applied in image domain to reconstruct the full dynamic image sequence for parameter estimation and parametric image generation.
Step 1. Sinogram Noise Normalisation: A PET scanner outputs the initial projection data in the form of N sinogram frames. This sinogram data is assumed to have been corrected for non-ideal physical scanner characteristics where necessary, e.g. PET data is typically attenuation-corrected. Each temporal sinogram frame is noise-normalized by multiplying by the square root of the total number of detected in the counts in the sinogram divided by the time interval covered by the frame - PCA is data driven technique that cannot itself distinguish noise from signal and so the frames are normalized to have approximately equal noise levels [8].
Step 2. Sinogram-domain PCA: The PCA is applied directly to the time series of N (noise-normalized) sinograms to produce a reduced number M of sinogram principal component (S-PC) channels. The PCA is performed simultaneously on the data from all spatial planes.

The objective of principal component analysis is to represent orthogonal maximum variance directions for the analysed data set. This multivariate image analysis method is well suited to high dimensional, highly correlated data such as dynamic PET data. If there are N frames in the CSS, PCA produces M principal components, $M \leq N$, where the eigenvalues of the PCA channels are ordered from largest to smallest.

Given a random vector population $X_{sinogram} = (x_1,\ldots, x_n)^T$,$x_1,\ldots x_n$ in this case represents the individual time samples of the dynamic tomographic study in the sinogram domain, and the mean vector of the population is defined as

$$\mu_{sinogram} = E\{ X_{sinogram} \} \quad (1)$$

and the covariance matrix is

$$C = E\{ (X_{sinogram} - \mu_{sinogram}) (X_{sinogram} - \mu_{sinogram})^T \} \quad (2)$$

,with eigenvalue-eigenvector pairs (λ_1 ,e_1), (λ_2 ,e_2)... (λ_n ,e_n). The eigenvectors are in the order of descending eigenvalues (largest first). To reduce the data set, only the first M eigenvectors are used to represent the data; the transformation of data vector $X_{sinogram}$ is derived as

$$\tilde{p} = A_{sinogram} (X_{sinogram} - \mu_{sinogram}) \quad (3)$$

where $\tilde{p}$ is a point in the orthogonal coordinate system defined by the eigenvectors. Components of $\tilde{p}$ can be seen as the coordinates in the orthogonal base. $A_{sinogram}$ is a

matrix consisting of first M eigenvectors of the covariance matrix as the row vectors.
Step 3. PCA Channel weighting: It is required that each PC in the M sinogram PCs is compressed with different quality according to their priority (importance of the signal) in the set of PCs. The PC channel with the higher priority requires less compression ratio.
Step 4. Sinogram-domain JPEG 2000:JPEG 2000 is applied to the each of M sinogram principal component channels with a weighted compression ratio to produce compressed M sinogram principal components.
Step 5. JPEG 2000 decoding: The decoding is performed on the M JPEG2000 compressed sinogram PCs to regenerate decompressed M sinogram PCs.
Step 6. PCA channel reconstruction:A set of M image principal component channels are reconstructed from the M decompressed sinogram PCs by using an image reconstruction algorithm such as filtered back projection (FBP) or ordered subset expectation-maximization (OSEM).
Step 7. Inverse PCA: The inverse of the PCA is performed on the M image principal component channels to regenerate a time series of N image frames.
In implementing the inverse PCA in the image domain, the PCA of the sinograms creates a transformation matrix $A_{sinogram}$ and a mean vector $\mu_{sinogram}$ (see eq. 1). The inverse PCA transformation in the image domain as required by step 7 is then-

$$\mathrm{Inv}(\tilde{p}) = (A_{sinogram})^{T} \times \tilde{p} + \mu_{sinogram} / \mathrm{NUM\_PROJ} \qquad (4)$$

where NUM_PROJ is the total number of projection angles in the tomograph.

4. Experiments

Simulation design: To validate this algorithm, a single slice of the brain Zubal phantom was used to simulate a dynamic PET brain study [5]. We inserted one synthetic tumour into lower left white matter. The activities in tumour, gray matter, and white matter were generated using a five-parameter four-compartment glucose tracer FDG model [9]. The conventional sampling schedule (CSS) for generating the tissue time activity curves (TTACs) is a set of intervals using the following scanning sequence: 10x 12 second scans, 2x0.5 minute scans, 2x1 minute scans, 1x1.5 minute scan, 1x3.5 minute scan, 2x5 minute scans, 1x10 minute scan and 3x 30 minute scans. The tissue time activity curves were then assigned to each brain region and a dynamic sequence of sinograms was generated by forward projecting the images into 3.13 mm bins on a 192 x 256 grid. To make the simulation data comparable to the expected real clinical data, we validated the noise level of the simulated model by comparing with that of clinical patient data- sinograms were scaled so that total counts were approximately 70M total counts for 31 planes over a one hour sample. Appropriate Poisson noise was added to each sinogram frame. For the per- regions-of-interest (ROI) experiments, to minimise partial volume effects, no blur was modelled, but for the per-pixel experiments blur of 5.8mm FWHM blur was simulated. Finally, dynamic sinograms were then reconstructed in a 128 x 128 matrix using filtered-back projection (FBP). For the ROI experiments, to avoid partial-volume effects, a ramp filter was used with the FBP, whereas for the per-pixel experiments a Shepp-Logan filter at 0.5 cps was used. Three ROI's were selected -

22 pixels for grey matter, 31 pixels for white matter and 10 pixels for tumour – to examine the accuracy and precision of parameter estimation by various methods.

Clinical studies: This algorithm was also evaluated on three clinical human brain FDG-PET studies- which were acquired by a SIEMENS ECAT 951R PET scanner, at the PET and Nuclear Medicine Department, Royal Prince Alfred Hospital, Sydney. The patients received an FDG infusion injection. A conventional sampling schedule (CSS) was used to acquire a dynamic sequence of 22 frames over 60 mins, which was 6x10s, 4x30s, 1x120s, and 11x300s. The PET data were decay-corrected and attenuation-corrected to the time of injection. Finally, dynamic sinograms were reconstructed in a 76 x 76 matrix using filtered-back projection with a Shepp-Logan filter with cutoff at 0.5 of the Nyquist frequency.

Evaluation: In this paper, for the per-ROI experiments, we used the percentage error of the estimated LCMRGlc mean and its coefficient of variation (CV) (which is defined as $CV = \sigma_K / \overline{K}$, Where K is a true parameter value, $\overline{K}$ is the mean of its estimates, σ_K is the standard deviation of the estimated parameter) to validate the performance of the various methods. For the per-pixel image-wide experiments, the criterion used to assess the validity of our technique was the mean square error (MSE). Compression Ratio (CR) was used as the measurement to assess compression efficiency, which is defined as $CR = t / L$, where t is the original file size, L is the compressed file size.

5. Results and Discussion

Figure 1 plots the mean squared error of the reconstructed images from the five sinogram PCA channels alone (S-PCA5), and followed by S-JPEG 2000 compression (S-PCA5 + S-JPEG2000) for patient 1, plane #16. The mean squared error slowly increases: even at a compression ratio of 100, the MSE is still less than 0.07. There is very minimum MSE up to a CR of 20. Normally each sinogram is approximately three times larger than its reconstructed image for PET brain studies, sinograms have more spatial redundancy and so are relatively easier to compress than reconstructed images.

Figure 2 gives a visual comparison of the reconstructed PCA channels from the S-PCA5 and S-PCA5 + S-JPEG2000 for patient 1, plane #16. The first PCA channel represents a weighted average of the component tissue time activity curves (TTACs) with largest eigenvalues, and the next few PCA channels represent tissues with significantly different TTACs with the decreasing amounts of variance. The higher channels are less important and so can tolerate a larger compression error. However, because S-PCA with noise normalization can't completely separate the signal from the noise, the eigenvalue of each channel isn't a good indicator of the importance of the signal in that channel. In this experiment the compression ratios for this experiment are chosen empirically based on the decreasing importance of the signal in the higher channels - CRs of 10:1, 33:1, 50:1, 100:1 and 100:1 for the first channel to fifth channel respectively. Future investigation of the optimal compression ratios for each S-PCA channel for accurate data analysis of dynamic PET is planned.

Presented in table I is the LCMRGlc parametric estimation comparison of S-PCA5, S-PCA5 followed by JPEG 2000 in sinograms (S-PCA5 + S-JPEG2000), and CSS methods for the simulated dataset. The ranking from best to worst for the averaged estimation error of LCMRGlc is S-PCA5 (1.38%), S-PCA5 + S-JPEG2000 (1.70%) and CSS (1.75%). The averaged values show S-PCA5 + S-JPEG2000 has the lowest CV for the estimated LCMRGlc (Ri) among all of the methods. The ranking for averaged coefficient of variation of Ri from best to worst is S-PCA5 + S-JPEG2000 (8.56%), S-PCA5 (8.95%), and CSS (14%).

Figure 3 plots the averaged results of the various approaches from table I. Figure 3(a) shows the error (%) results of the Ri estimates averaged over gray matter, white matter, and tumour, for various methods. Figure 3(b) plots the corresponding CVs of the Ri.

Figure 4 shows the parametric images of LCMRGlc based on a pixel-by-pixel estimation using CSS, S-PCA5 and S-PCA5 + S-JPEG2000 for the simulated dataset. Figure 4(a) is the original last frame of plane #16 of CSS. Figures 4 (b) –(d) show the parametric images from CSS, S-PCA5 and S-PCA5 + S-JPEG2000 respectively. The parametric image is relatively noisy using CSS compared with S-PCA5 and S-PCA5 +S-JPEG2000. The mean squared error is used to validate the performance of CSS and S-PCA in terms of the parametric image generation against the ground truth (parametric image generated from noise free simulated data set). The MSE for CSS is approximately three times that of S-PCA5 + S-JPEG2000. MSE is 0.9763, 0.4331 and 0.3258 for CSS, S-PCA5 and S-PCA5 + S-JPEG2000 respectively. Note: the MSE values calculated exclude the outside of the brain. For the simulation experiments, the results shown in table I and figures 3 and 4 indicate that our proposed compression method can reduce the noise and improve the accuracy and precision for parametric estimation compared with the original data.

Figure 5 shows plane #20 of the dynamic reconstructed PET series for patient 3. The first row shows the eleventh, thirteenth, fifteenth, nineteenth and the final frame of original 22 frames of CSS; The second row contains the corresponding reconstructed images from the S-PCA5; The last row shows the corresponding reconstructed images from S-PCA5 + S-JPEG2000. The signal-to-noise ratio (SNR) of the reconstructed images from S-PCA5 and S-PCA5 + S-JPEG2000 is significantly improved. It is noted that the reconstructed images from S-PCA5 + S-JPEG2000 are slightly less noisy than that from S-PCA5, because JPEG2000 itself has a denoising effect. The results indicate that S-PCA5 + S-JPEG2000 not only can reduce the quantity of data in dynamic PET, but also improved the image quality of PET.

Figure 6 gives a visual comparison of the parametric images based on a per-pixel estimation of LCMRGlc for CSS, S-PCA5 and S-PCA5 + S-JPEG2000 on one plane for two clinical datasets. The first column of images are the results obtained from CSS; the second column of images are the corresponding results from S-PCA5; the last column of images are the corresponding results from S-PCA5 + S-JPEG2000. Once again the results show the noise reduction achieved with S-PCA5 and S-PCA5 + S-JPEG2000 compared with CSS. The better precision of the S-PCA5 + S-JPEG2000 estimation is evident from the less noisy images, and there are fewer pixels that failed to converge to an estimate.

Table II illustrates the performance of the proposed compression technique. In step one, the use of S-PCA5 to reduce the dimensionality of the data from typically 22 to

5 temporal frames provided a CR of 4.4:1. In step two, the five sinogram principal component channels were further compressed spatially by JPEG 2000, which gives an average compression ratio of 29.4:1. Finally the global compression ratio is approximately 130:1.

6. Conclusion

In this paper, we have investigated a new approach to dynamic PET data compression by temporal compression by sinogram-domain principal component analysis followed by spatial compression by applying JPEG2000 to the PCA sinograms. Using a simulated phantom FDG brain study and three clinical studies, we evaluated the fidelity of the compressed data for estimation of local cerebral metabolic rate of glucose by a four-compartment model. The results indicate that this proposed compression technique not only can greatly reduce the quantity of data in dynamic PET, but also can improve the image quality of PET for quantitative analysis, while preserving the sinogram data for later analysis.

Acknowledgments:
This research is partially supported by ARC and HK-RGC grants.

References

1. K V Mardia, J T Kent and J M Bibby, "Multivariate Analysis", New York: Academic, pp.224, 1979.
2. Z. Chen, B.Parker, D.D.Feng, "Temporal Compression of Dynamic Positron Emission Tomography via Principal Component Analysis in the Sinogram Domain,"*IEEE Medical Imaging Conference*, October 19-25, 2003, Portland, Oregon, U.S.A.
3. V. Chameroy & R. D. Paola, " High compression of nuclear medicine dynamic studies", *International Journal of Cardiac Imaging* 5: 261-269, 1990.
4. T. Kao, S.H. Shieh, and L.C. Wu, "Dynamic Radionuclide Images Compression Based on Principal Components Analysis," *Engineering in Medicine and Biology Society*, Vol.3, pp. 1227 –1228, 1992.
5. I.G Zubal, C.R. Harrell, E.O. Smith, Z. Rattner, G. Gingi, and P. B. Hoffer, " Computerized three-dimensional segmented human anatomy", *Med. Phys. 21:299-302.*
6. S.C. Huang, M.E. Phelps, E.J. Hoffman, K. Sideris, C. Selin, and D.E. Kuhl, "Non-invasive determination of local cerebral metabolic rate of glucose in man", *Amer. J. Physiol.*, vol. 238, pp.E69-E82, 1980.
7. D. Feng, D. Ho, K. Chen, LC. Wu, J-K. Wang, R-S. Liu and S-H. Yeh, "An Evaluation of the Algorithms for Determining Local Cerebral Metabolic Rates of Glucose Using Positron Emission Tomography Dynamic Data", *IEEE Transactions on Medical Imaging*, Vol. 14, No. 4, December 1995.
8. F. Pedersen, M. Bergstrom, E. Bengtsson, B.Langstrom, "Principal component analysis of dynamic PET and Gamma Camera Images: A methodology to visualize the signals in the presence of large noise", *1993 IEEE conference record Nuclear Science Symposium and Medical Imaging Conference*. San Francisco, Calif. 1993, Vol. 3, pp.1734-1738.

9. R.A. Hawkins, M.E. Phelps, and S.C. Huang, " Effects of temporal sampling, glucose metabolic rates, and disruptions of the blood-brain barrier on the FDG model with the without a vascular compartment: Studies in Human brain tumors with PET", *J.Cereb. Blood Flow Metab.* 6:170-183,1996

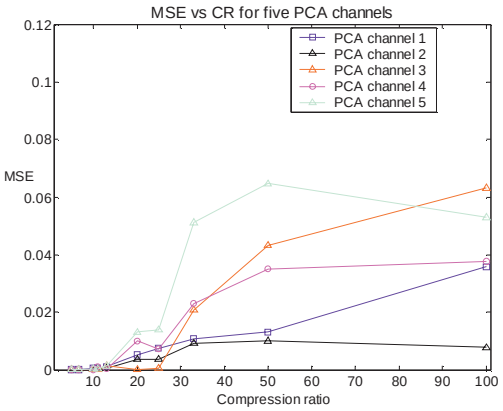

Figure 1. Mean squared errors of 5 PCA channels reconstructed from S-PCA5 + S-JPEG2000 for patient, 1 plane #16

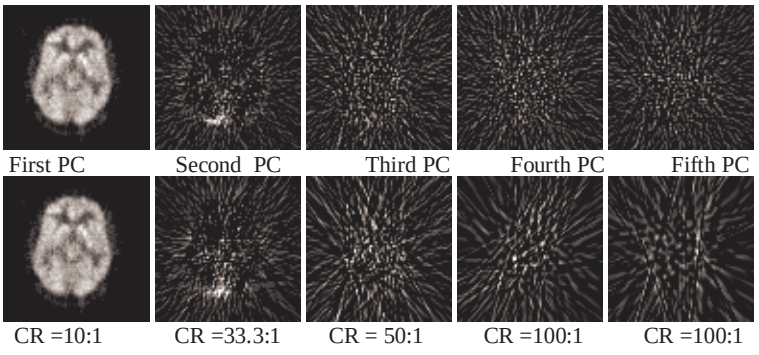

Figure 2. Top row shows the five PCA channels reconstructed from S-PCA5 and bottom row shows the corresponding five PCA channels reconstructed from S-PCA5 + S-JPEG2000 for patient 1, plane #16.

	Error (%) of LCMRGLc (Ri)			CV (%) of LCMRGLc (Ri)		
ROI	CSS	SPCA5	SPCA5 +SJPEG2000	CSS	SPCA5	SPCA5 +SJPEG2000
Gray matter	3.55	0.55	1.53	9.61	5.56	5.09
White matter	0.56	2.68	3.28	16.01	10.57	10.14
Tumour	1.14	0.91	0.30	16.41	10.71	10.44
Averaged	1.75	1.38	1.70	14.01	8.95	8.56

Table I. Comparison of percentage Error and CV's of LCMRGLc (Ri) for the simulated dataset (100 runs).

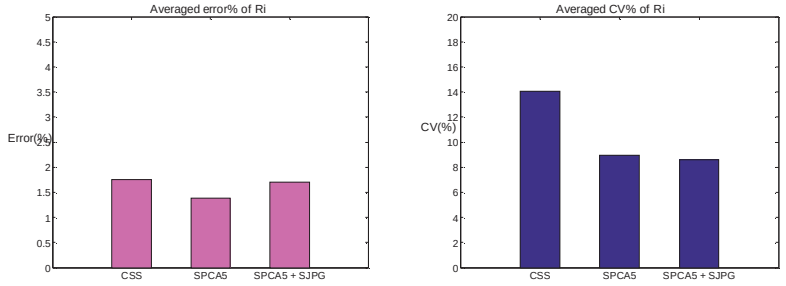

(a) (b)

Figure 3. Comparison of accuracy and precision of estimation for LCMRGLc (Ri) by different methods - CSS, S-PCA5, S-PCA5 + S-JPEG2000 (SPCA5 + SJPG) for the simulated dataset. Fig. 3 (a) Averaged estimated errors (%) of Ri. Fig.3 (b) Averaged CV (%) of Ri for the simulated dataset.

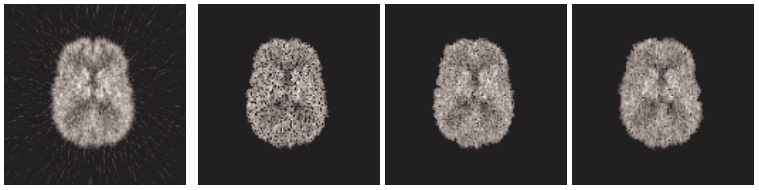

(a)Final frame (b) Ri from CSS (c) Ri from S-PCA5 (d) Ri from S-PCA5 + S-JPEG2000

Figure 4. Comparison of parametric images of LCMRGLc(Ri) formed with CSS, S-PCA5 and S-PCA5 + S-JPEG2000 (pixel-by-pixel approach) from simulated data (plane #16) with clinical noise and blur. The parametric image from CSS with the MSE of 0.9763. The last two images are parametric images from S-PCA5 and S-PCA5 + S-JPEG2000 and MSE is 0.4331 and 0.3258 respectively.

	Data set	CR
Original	22 frames	1.0:1.0
S-PCA5	5 PCA channels	4.4:1
S-JPEG 2000	5 compressed PCA channels	29.4 :1
S-PCA5 + S-JPEG2000		129.4 :1

Table II. Compression ratios for the simulated dataset and three clinical datasets.

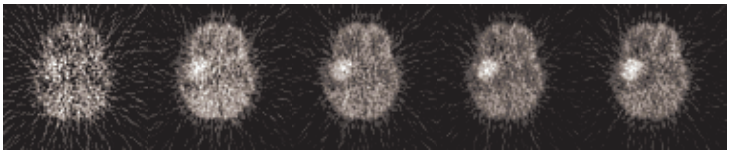

(a) Dynamic images reconstructed from original 22 sinograms of CSS

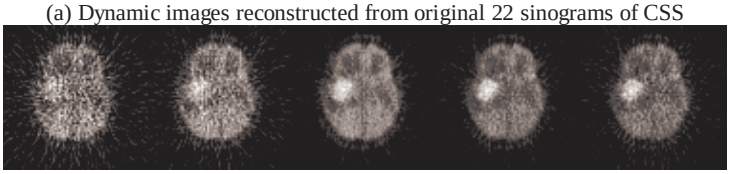

(b) Dynamic images reconstructed from S-PCA5

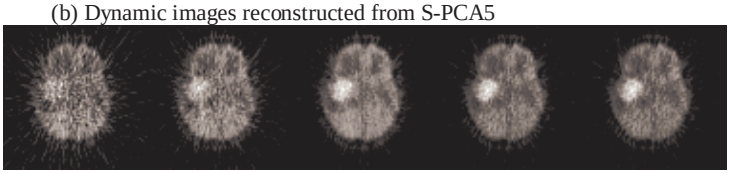

(c) Dynamic images reconstructed from S-PCA5 + S-JPEG2000

Figure 5. Dynamic reconstructed PET series for clinical patient 3, plane #20. Fig .5 (a). Frames 11,13,15,17, 19 and 22 from the original 22 sinograms of CSS. Fig 5(b). Corresponding reconstructed frames from S-PCA5. Fig.5 (c) Corresponding reconstructed frames from S-PCA5 + S-JPEG2000. Each image is scaled by its own maximum.

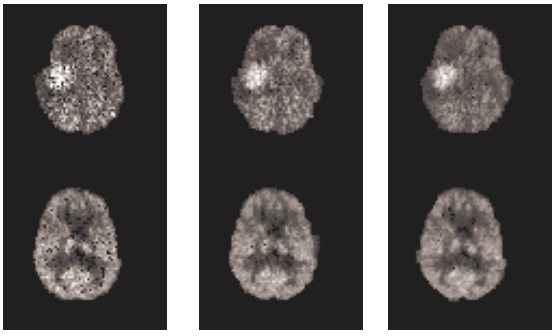

Figure 6. Comparison of parametric images of Ri formed with CSS, with S-PCA5 and with S-PCA5 + S-JPEG2000 based on pixel-by-pixel approach from patient 3,plane #20, patient 2,plane #16. The first column shows the parametric images from CSS. The second column shows the corresponding parametric images from S-PCA5. The third column shows the corresponding parametric images from S-PCA5 + S-JPEG2000. Note: The black spots are unconverged pixels.